Plasma Phys. Control. Fusion **38** (1996) 1805–1816. Printed in the UK

A new scheme for heterodyne polarimetry with high temporal resolution

J H Rommers† and J Howard‡

† FOM–Instituut voor Plasmafysica, Association Euratom-FOM, PO Box 1207, 3430 BE Nieuwegein, The Netherlands

‡ Plasma Research Laboratory, Australian National University, Canberra ACT 0200, Australia

Received 3 May 1996, in final form 14 June 1996

Abstract. A new scheme for making combined interferometric and polarimetric measurements on tokamak plasmas with high temporal resolution is presented. The method, which can be regarded as a generalization of techniques suggested by other workers, can achieve bandwidths in excess of 100 kHz using an optically pumped far-infrared triple laser source. A bandwidth of 10 kHz with an accuracy of better than 0.2° has already been demonstrated. Calibration measurements as well as first plasma measurements obtained with the new approach are presented and evaluated.

1. Introduction

The current density distribution in tokamak plasmas plays a crucial role in determining the plasma equilibrium and its stability. Provided that the shape of the outer flux surfaces is known, the poloidal field distribution can be determined from a measurement of the Faraday rotation of the plane of polarization of far-infrared laser radiation transmitted through the plasma (polarimetry). Since this poloidal field distribution is determined by a combination of plasma current and currents in external equilibrium coils, one is then able to reconstruct the current density profile in the plasma. Other methods, such as the measurement of the Zeeman splitting of ionic energy levels, tangential Thomson scattering, or the motional Stark effect have also been attempted, but only the latter is used routinely at present.

Many schemes have been proposed for the difficult measurement of the small Faraday rotation angles typical for tokamak plasmas [1]. One of the simplest and most successful methods was implemented by Soltwisch on the TEXTOR tokamak [2]. Here, the orthogonal electric field component due to the Faraday rotation of an initially linearly polarized laser beam is transmitted (or reflected) by an analysing wire grid polarizer. A measurement of the relative power in the reflected and transmitted components is used to determine the Faraday rotation angle. The rotation of the electric vector arises because of the difference between the phase velocities of the two counter-rotating and approximately circularly polarized characteristic waves that propagate parallel to $\boldsymbol{B}$ in a magnetized plasma. A method for sensing this phase difference directly has been proposed and demonstrated by Howard [3]. In both these cases, a simple plane polarized wave is injected into the plasma and two detectors are required to extract the average (interferometric) phase ϕ and the (polarimetric) phase difference α_{F} imparted on the probing beam.

More sophisticated techniques actively modulate the polarization vector, before directing it through the plasma. This offers the advantage of using a single detection element for

0741-3335/96/101805+12$19.50

each probing channel, which considerably simplifies the optical setup and hence can be regarded as an almost essential requirement in expanded or multi-beam systems. The use of a rocking polarization vector was suggested by Kunz and Dodel [4]. This method suffers from high laser power losses in the ferrite modulating element. Dodel and Kunz [5] also proposed a scheme where left- and right-handed circularly polarized beams (at slightly offset frequencies) are superimposed and launched into the plasma. The transmitted rotating linearly polarized wave is passed through an analyser and detected to give an oscillating signal at the difference frequency that suffers a phase retardation proportional to the Faraday angle. With this method of optical processing, a second detector is required for the measurement of ϕ (contaminated by α_F) and one of the essential advantages of the method is lost.

A more refined scheme that allows the use of a single detector for both the interferometric and the polarimetric measurement was proposed and successfully implemented by Rice [6] at MTX. In this arrangement, a rotating elliptically polarized wave is generated mechanically using a rotating half-wave plate. The probing wave is sent through a polarizer before being combined with a frequency-offset local oscillator on a detector. An amplitude-modulated (AM) intermediate-frequency (IF) carrier signal is obtained. The phase of the carrier conveys ϕ and the phase of the modulation of the envelope α_F. Because of the non-zero ellipticity, the detector signal is never completely extinguished and ϕ and α_F can be recovered using standard electronic demodulation methods. As with the Dodel and Kunz method, the interferometer signal also suffers some crosstalk from α_F [7]. A common problem with methods that rely on mechanical modulation of the laser polarization is the limited IF bandwidth ($\lesssim$10 kHz).

In this paper we propose a single-detector scheme, that can be regarded as a generalization of both the Dodel–Kunz and the Rice methods discussed above. We introduce a new method of data analysis that both ameliorates the crosstalk problems of these methods and, apart from signal-to-noise-based restrictions on the bandwidth, allows for a very high temporal resolution.

2. Method description

If the typical gradient lengths in the plasma are much larger than the wavelength considered, the dispersion relation for propagation of an electromagnetic wave in a plasma can be described by the well known Appleton–Hartree formula. In a magnetized plasma, the solution for the refractive index gives two orthogonal polarization eigenstates (characteristic waves) that propagate with different phase velocities. When the angle between the direction of propagation of the electromagnetic wave and the external magnetic field is not too close to 90°, these two eigenstates are, for usual interferometer wavelengths, counter-rotating and approximately circularly polarized. The Faraday rotation of the plane of polarization of an incident linearly polarized wave is caused by the difference in phase velocity of these circularly polarized eigenstates, and so is equal in magnitude to half the phase difference between the characteristic waves after traversing the plasma.

Previous methods have aimed at measuring the angle over which the incident polarization (which may also be elliptical, as in the Rice scheme) is rotated by the plasma. In the approach described here (see figure 1) we measure the line-averaged refractive indices of the characteristic waves involved directly, by injecting two co-aligned counter-rotating circularly polarized laser beams into the plasma. The beams, which are generated by separate far-infrared lasers with frequencies ω_1 and ω_2, are slightly frequency offset ($|\omega_2 - \omega_1| \sim$ a few hundred kHz) to allow the use of heterodyne detection methods.

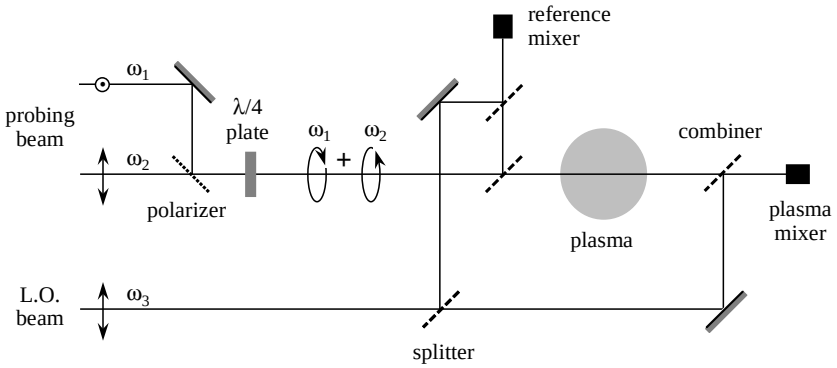

Figure 1. Schematic depiction of the polarimeter setup suggested by the authors. Two laser beams with angular frequencies ω_1 and ω_2 are transmitted through the plasma in orthogonal circular polarization states. Co-alignment of the two beams is achieved without power loss using a polarizer/quarter wave plate combination. A third laser at frequency ω_3 acts as local oscillator for heterodyne detection of the interferometric phase shift.

At far-infrared frequencies, direct measurement of the phases of the probing beams is not feasible. By inserting a polarizer in front of the non-linear detector (mixer), a signal at the difference frequency $|\omega_2 - \omega_1|$ is obtained. Upon comparison with the phase of a similarly generated reference signal (without plasma), the phase difference between the two probing beams (corresponding to twice the Faraday rotation angle) is obtained. This polarimetric measurement principle is similar to that proposed by Dodel and Kunz [5].

To simultaneously obtain the interferometric phase shift (which is the average phase shift of the independent characteristic waves) the authors suggest not using a second detector, as in the original Dodel and Kunz scheme, but mixing the two probing beams with an additional local oscillator (LO) at frequency ω_3. The spectrum of the detected signal in this case consists of three intermediate frequency (IF) carriers corresponding to the mixing product between the two probes ($|\omega_2 - \omega_1|$) and those between each of the probes and the local oscillator ($|\omega_1 - \omega_3|$ and $|\omega_2 - \omega_3|$). Similar signals are generated in a reference interferometer unaffected by the plasma. The interferometric phase can be obtained from the average of the phase changes registered by the two probe–LO carriers with the difference between the two phase angles being equal to twice the Faraday angle α_F. The Faraday rotation can also be deduced directly from the mixing product between the two probing waves, as is done in the Dodel–Kunz scheme. Since the phase of the mixing product is independent of the power in each of the constituent beams, the requirement of equal power, as posed by Dodel and Kunz, is in fact unnecessary. Obviously, the situation of equal beam powers is desirable from the point of view of measurement accuracy.

3. Complication owing to non-circularity of the polarization eigenstates

For experiments in a toroidally confined plasma, the helical magnetic geometry implies that the polarization eigenstates are generally not perfectly circularly polarized. To accommodate this, let the polarization eigenstates of the characteristic waves be denoted by

$$\boldsymbol{E}_{(1)} = \frac{1}{\sqrt{1+\alpha^2}} \begin{pmatrix} 1 \\ \mathrm{j}\alpha \end{pmatrix} \qquad \boldsymbol{E}_{(2)} = \frac{1}{\sqrt{1+\alpha^2}} \begin{pmatrix} \alpha \\ -\mathrm{j} \end{pmatrix} \tag{1}$$

with associated refractive indices obtained from the Appleton–Hartree formula:

$$N_{(1)}^2 = 1 - \frac{(\omega_\mathrm{p}\omega^{-1})^2}{1 - \alpha\omega_{\mathrm{c,e}}\omega^{-1}\cos\theta} \qquad N_{(2)}^2 = 1 - \frac{(\omega_\mathrm{p}\omega^{-1})^2}{1 + \alpha^{-1}\omega_{\mathrm{c,e}}\omega^{-1}\cos\theta}. \quad (2)$$

Here, ω is the wave angular frequency, $\omega_{\mathrm{c,e}}$ and ω_p are the electron cyclotron angular frequency and the plasma angular frequency, respectively, and θ denotes the angle between the magnetic field and the propagation direction of the wave. The polarization parameter α, which is related to the ellipticity of the eigenstate,

$$\alpha = -\mathrm{j}\frac{E_{y(1)}}{E_{x(1)}} = -\mathrm{j}\frac{E_{x(2)}}{E_{y(2)}} \quad (3)$$

can, without loss of generality, be restricted to the interval $[-1, 1]$. The two propagation eigenstates are circular for $\alpha = \pm 1$ and linear for $\alpha = 0$. In figure 2 the result of a numerical calculation of α in a poloidal plasma cross section is shown for a typical discharge of the RTP tokamak (see section 5 for a short description of RTP), demonstrating that the polarization eigenstates are not at all circular.

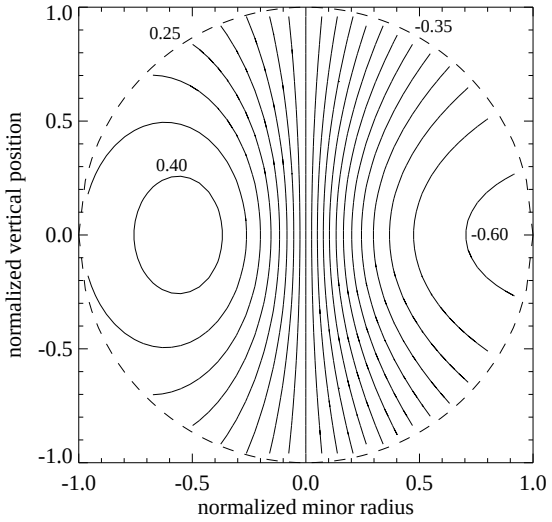

Figure 2. Value of the ratio α, describing the polarization of the propagation eigenstates in the RTP plasma, in the case of a vertically propagating wave of 693 GHz. A parabolic density profile and a Kadomtsev-like current density profile [12] have been assumed. The asymmetry is caused by the dependence of the toroidal magnetic field on the major radius. The peak density is taken to be 5×10^{19} m^{-3}, the total current is 100 kA ($q_a = 4.0$).

The change of polarization state of a beam propagating through a homogeneous plasma slice of thickness dz can be described using the plasma Jones matrix **P** given by [8–10]

$$\mathbf{P} = \begin{pmatrix} \cos\frac{\mathrm{d}\psi}{2} + \mathrm{j}\frac{1-\alpha^2}{1+\alpha^2}\sin\frac{\mathrm{d}\psi}{2} & \frac{2\alpha}{1+\alpha^2}\sin\frac{\mathrm{d}\psi}{2} \\ -\frac{2\alpha}{1+\alpha^2}\sin\frac{\mathrm{d}\psi}{2} & \cos\frac{\mathrm{d}\psi}{2} - \mathrm{j}\frac{1-\alpha^2}{1+\alpha^2}\sin\frac{\mathrm{d}\psi}{2} \end{pmatrix} \mathrm{e}^{-\mathrm{d}\phi}. \quad (4)$$

Here, the poloidal field is assumed to be in the y–z plane and wave propagation is along the z-axis. dψ and dϕ are directly related to the difference between the refractive indices of the two eigenstates $\Delta N = N_{(1)} - N_{(2)}$, and their average $\bar{N} = (N_{(1)} + N_{(2)})/2$, respectively:

$$\mathrm{d}\psi = \frac{\omega}{c}\Delta N\,\mathrm{d}z \qquad \mathrm{d}\phi = \frac{\omega}{c}\bar{N}\,\mathrm{d}z. \quad (5)$$

The velocity of light in vacuum is denoted by c.

When the propagation eigenstates have circular polarization ($\alpha = \pm 1$), the plasma matrix reduces to a simple rotation matrix with (Faraday) rotation angle $\mathrm{d}\psi/2$. The situation is more complicated when the eigenstates are not circularly polarized, with the Faraday rotation no longer being simply proportional to the difference in refractive indices. If the incident wave is linearly polarized and the Faraday angle is determined from the amount of power that converts to the orthogonal state, it is well established that, for small angles $\mathrm{d}\psi$, the Faraday angle is given by [11]

$$\mathrm{d}\alpha_{\mathrm{F}} = \frac{2\alpha}{1+\alpha^2}\frac{\mathrm{d}\psi}{2} = \frac{1}{2}\Big(\frac{\omega_{\mathrm{p}}}{\omega}\Big)^2 \frac{\omega_{\mathrm{c,e}}}{\omega}\cos\theta\frac{\omega}{c}\mathrm{d}z. \tag{6}$$

To calculate the change in polarization state for an elliptically polarized input wave, however, we need to make use of the plasma matrix. Consider an incident wave having its major ellipse axis tilted by an angle ξ relative to the x-axis of the laboratory frame and with ellipticity ε, such that

$$\boldsymbol{E}_{\mathrm{inc}} = \begin{pmatrix} \cos\xi + \mathrm{j}\sin\xi \\ \sin\xi - \mathrm{j}\cos\xi \end{pmatrix} \exp[-\arctan(\varepsilon\tan\xi)] \tag{7}$$

where the exponent is chosen to make the initial phase of the wave along the detection axis independent of ξ. We assume that, after passage through the homogeneous plasma slab, only the polarization component parallel to the toroidal magnetic field is detected. The phase $\mathrm{d}\Phi$ of this component relative to the mean phase shift $\mathrm{d}\phi$ can be calculated by applying (4) to obtain

$$\mathrm{d}\Phi = \arctan\left(\frac{\big(\frac{1}{2}(1-\alpha^2)[(1-\varepsilon^2)\cos 2\xi - (1+\varepsilon^2)] + 2\alpha\varepsilon\big)\tan(\mathrm{d}\psi/2)}{(1+\alpha^2)(\sin^2\xi + \varepsilon^2\cos^2\xi) - \alpha(\varepsilon^2-1)\sin 2\xi\tan(\mathrm{d}\psi/2)}\right) - \mathrm{d}\phi. \tag{8}$$

This equation is rather obscure, but can be simplified significantly by realizing that the angle $\mathrm{d}\psi/2$ is small, and by assuming that the ellipticity of the incident wave is close to unity, i.e. $\varepsilon = \pm(1-\Delta\varepsilon)$, with $\Delta\varepsilon$ small and positive. Neglecting quadratic terms in $\Delta\varepsilon$ one may simplify (8) to yield

$$\mathrm{d}\Phi = \frac{\alpha^2 - 1 \pm 2\alpha[1 + \Delta\varepsilon\cos 2\xi]}{1+\alpha^2}\frac{\mathrm{d}\psi}{2} - \mathrm{d}\phi \tag{9}$$

The phase difference $\Delta(\mathrm{d}\Phi)$ between two orthogonally polarized waves with ellipticities $(1-\Delta\varepsilon_1)$ and $-(1-\Delta\varepsilon_2)$ is therefore given by

$$\Delta(\mathrm{d}\Phi) = \frac{2\alpha}{1+\alpha^2}[2 + \Delta\varepsilon_1\cos 2\xi_1 + \Delta\varepsilon_2\cos 2\xi_2]\frac{\mathrm{d}\psi}{2} \tag{10}$$

and is proportional to the usual Faraday rotation angle given in (6). When the probing waves are not exactly circular, the fractional error term is less than or equal to half the sum of the two deviations, depending on the exact orientations of the polarization ellipses.

It is concluded that measurement of the phase difference between two counter-rotating circularly polarized waves injected into the plasma is a reliable measure of the Faraday rotation angle α_{F}, even though the eigenstates in the plasma are not at all circular. Although care needs to be taken to ensure that the polarizations of the probing beams are sufficiently close to circular, it is not essential that they be of equal power.

4. Relation to the Rice scheme

The scheme proposed in this paper is closely related not only to the Dodel–Kunz scheme, but also to the method used by Rice [6] and illustrated in figure 3. The rotating polarization ellipse used in the Rice method can be regarded as the superposition of two elliptically polarized, frequency-offset waves. This insight suggests a new method for data analysis that exploits this decomposition of the rotating ellipse.

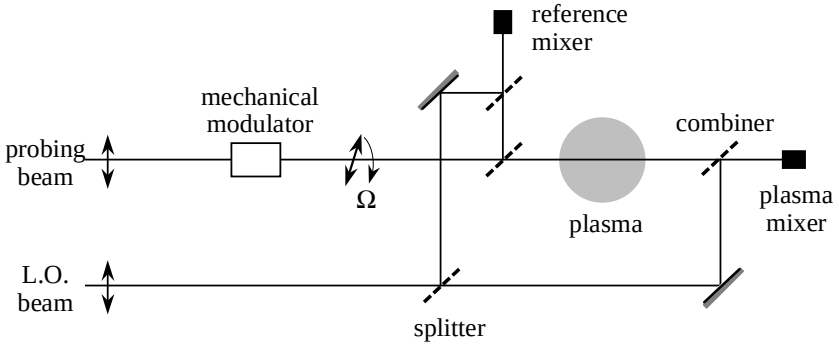

Figure 3. Schematic depiction of the rotating elliptical beam setup as implemented by Rice.

To generate the elliptically polarized far-infrared beam, the laser radiation is passed through an adjustable birefringent plate followed by a rotating half-wave plate. The resulting polarization ellipse rotates at twice the angular frequency of the half-wave plate. To express the resulting polarization state mathematically, it is assumed for convenience that the major axis of the polarization ellipse of the incident wave is oriented parallel to the x-axis of the laboratory frame. After passage through the plasma the electric vector will be rotating at angular frequency Ω due to the wave-plate rotation and will have suffered a Faraday rotation α_F and a phase retardation ϕ due to the plasma. The resulting polarization vector $\boldsymbol{P}$ can be represented using Jones matrices as

$$\boldsymbol{P} = \begin{pmatrix} \cos(\Omega t + \alpha_F) & \sin(\Omega t + \alpha_F) \\ \sin(\Omega t + \alpha_F) & -\cos(\Omega t + \alpha_F) \end{pmatrix} \begin{pmatrix} \cos(\omega_0 t + \phi) \\ \varepsilon \sin(\omega_0 t + \phi) \end{pmatrix} \tag{11}$$

where ω_0 is the angular frequency of the radiation and ε is the ellipticity introduced by the birefringent plate.

On emerging from the plasma the beam passes through an analyser that selects a single polarization component, here taken, without loss of generality, to be the x-component. Subsequent mixing with a local oscillator shifts the carrier down to a more easily detectable intermediate frequency ω. Using some involved, but straightforward manipulations, it is possible to express the detector signal S as the product of an oscillating envelope, phase modulated by α_F, and a carrier at frequency ω that conveys the interferometric phase ϕ:

$$S = \sqrt{\frac{\varepsilon^2+1}{2}} \sqrt{1 - \frac{\varepsilon^2-1}{\varepsilon^2+1} \cos(2\Omega t + 2\alpha_F)} \times \cos(\omega t + \arctan[\varepsilon \tan(\Omega t + \alpha_F)] + \phi). \tag{12}$$

In the approach taken by Rice, the envelope and carrier are electronically separated and phase demodulated. When the ellipticity is non-zero, the amplitude never vanishes, enabling in principle relatively high time-resolution measurements of the carrier phase. One limitation

of the method, however, is evident in the presence of the polarimetric 'crosstalk' term in the expression for the phase. Although this can be removed by filtering the interferometer signal, the interferometer time resolution will be severely compromised. Since all three quantities involved in the crosstalk are known (ε and Ω) or measured (α_F), one can in principle correct the interferometer data for the polarimetric component. In practice, however, this is extremely difficult because of uncertainties in the parameters. Even with a reference signal (that does not encounter the plasma), the ellipticity term (at harmonics of Ω) is difficult to compensate exactly.

The modulated beat signal described by (12) can be more simply represented using (11) in the alternative form

$$S = \frac{1-\varepsilon}{2}\cos([\omega+\Omega]t+\phi+\alpha_F) + \frac{1+\varepsilon}{2}\cos([\omega-\Omega]t+\phi-\alpha_F). \quad (13)$$

This shows that the detected signal is composed of two intermediate-frequency carriers at $\omega-\Omega$ and $\omega+\Omega$ corresponding to the superposition of the left- and right-hand elliptically polarized components generated by the modulator. Observe now that both interferometric and polarimetric phases can be unambiguously recovered provided only that $\varepsilon \neq \pm 1$. This suggests that the Faraday rotation and the interferometer phase shift can be obtained by performing separate phase measurements on the two carriers as in the scheme proposed here. The signal bandwidth is limited by the separation of the carriers and therefore by the rotation speed of the modulator. Because of the crosstalk term in (12), this is essentially also the case for the analysis scheme used by Rice.

5. Experiment

The RTP tokamak ($R_0 = 0.72$ m, $a = 0.164$ m, $I_p \leqslant 150$ kA, $B_t \leqslant 2.4$ T) is equipped with a heterodyne FIR interferometer/polarimeter operating at 432.5 μm. Three separate cavities, pumped by a single CO_2 laser, are used to generate two probing beams and a local oscillator beam. Upon exiting the laser, the two probing beams are co-aligned, and the beam polarizations are set to counter-rotating circular. The probing beams are expanded using parabolic optics to fill the RTP ports and up to 19 Schottky diode corner cube mixers are used for polarization-sensitive detection of the slab beam. The width of the laser transition allows frequency offsets (IF) of the order of several MHz to be obtained by slightly detuning the relative cavity lengths. For combined interferometry and polarimetry the method as discussed in section 2 and depicted in figure 1, has been implemented.

The measured signals are acquired directly at a digitization rate of 500 kHz without any electronic signal processing other than amplification and bandpass filtering (0.1–5 MHz). For the data presented here, the probe–probe mixing frequency was set to approximately 550 kHz and one of the probe–LO mixing frequencies to 625 kHz, causing the second probe–LO mixing peak to reside at approximately 1175 kHz. Since these frequencies are higher than the Nyquist frequency of the digitizers, the sampled signals are aliased on digitization. The laser frequencies, however, are chosen such that this does not cause loss of information. For each detector the three carriers can be isolated using numerical bandpass filters and the phases extracted by comparing the corresponding computed analytic signals [3].

For instrument calibration, a stepper-motor-driven rotating half-wave plate can be inserted in the probing arm (before beam expansion). In this way the linear polarization angle can be incremented in small steps of $\sim 0.7^\circ$ to test the polarimeter resolution. Measured rotation angles are shown in figures 4 and 6 for many detectors at 2 kHz and for a single detector at 10 kHz, respectively. A statistical analysis of the measurement accuracy

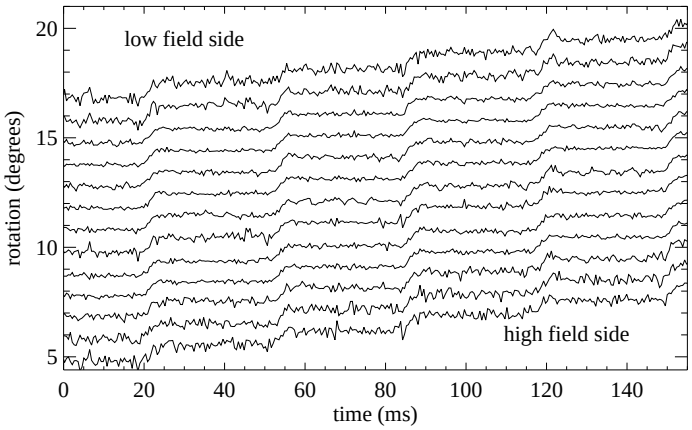

Figure 4. Calibration traces for all channels then in operation. A half-wave plate, rotated by a stepper motor, was used to rotate the polarization of the incident waves over 0.7°. The data were taken with a temporal resolution of 2 kHz.

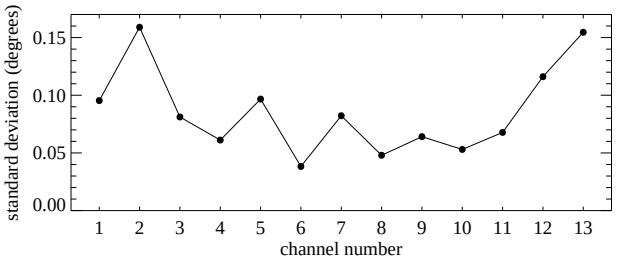

Figure 5. Standard deviation of each of the signals, shown in figure 4. The standard deviation was derived from a statistical analysis extending over one whole flat period, *in casu* [80, 105] ms. Except for two less sensitive detectors, the standard deviation increases towards the edges of the beam profile because of decreased signal levels.

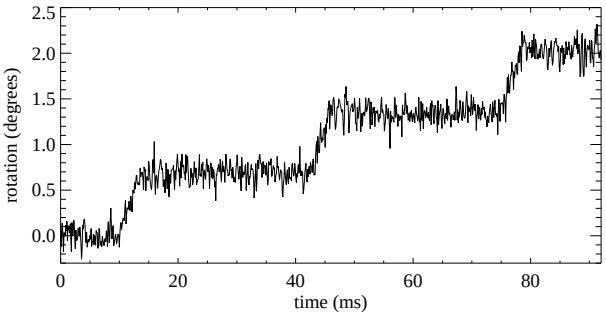

Figure 6. Calibration trace for a single detector, demonstrating the high temporal-resolution capability of the system. The data were filtered with a low-pass filter at 10 kHz.

demonstrates that the standard deviation at 2 kHz is of the order of 0.05° for most lines of sight (see figure 5). The degraded accuracy in the edge (see figure 5) channels is the result of a decrease in signal power both because of the beam profile and because of a narrowing of the access ports towards the (high-field) side. Figure 6 demonstrates the high temporal-

resolution capability of the method, with a measurement error of less than 0.2° at 10 kHz. Since the temporal resolution is in principle limited only by the laser gain bandwidth, fast plasma events (such as sawteeth or other MHD activity) can be studied at high temporal resolution. If the perturbation amplitude is small one can use coherent addition techniques to improve the signal-to-noise level provided the MHD events have a sufficiently constant periodicity.

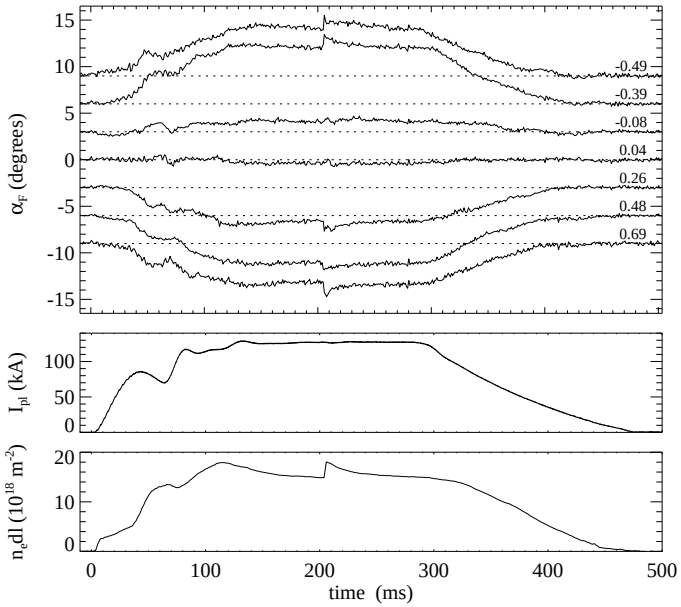

Figure 7. Faraday rotation time traces at 1.0 kHz for an ohmic discharge, in which a small pellet has been injected at 200 ms. The normalized channel positions are indicated. The channels are offset from zero for plotting purposes. The line-integrated density and the plasma current are given for reference.

An example of the measured Faraday rotation signals during an ohmic hydrogen discharge is given in figure 7. A pellet is injected into the plasma at 200 ms, leading to an increase in density and hence in Faraday rotation. Depending on signal-to-noise considerations, either the phase of the probe–probe mix or, alternatively, the phase difference between the two probe–LO mixes is used to calculate the Faraday rotation angles. Apart from a difference in signal-to-noise ratio, figure 8 illustrates the equivalence of the two alternatives. Evidently, a signal-to-noise-weighted combination of the two could be calculated to further improve the measurement accuracy.

For the above discharge, both a line-integrated density profile and a Faraday rotation profile are plotted in figure 9 for the time point $t = 200$ ms. A parametrization procedure has been used to simultaneously derive a density profile from the line-integrated density measurement and a current profile from the Faraday rotation measurement. Because of the high density, and the long distance between plasma midplane and detector position, refraction effects have been included in the parametrization.

The class of density profiles in the parametrization was taken to be $(n_0-n_a)(1-\rho^\beta)^\gamma+n_a$, where ρ is the normalized radius of the flux surfaces, and n_0 and n_a are the central and edge density respectively. Outside the limiter radius, an exponential decay with a 1/e length of 4 mm has been assumed. This set of profiles suffices to describe adequately all

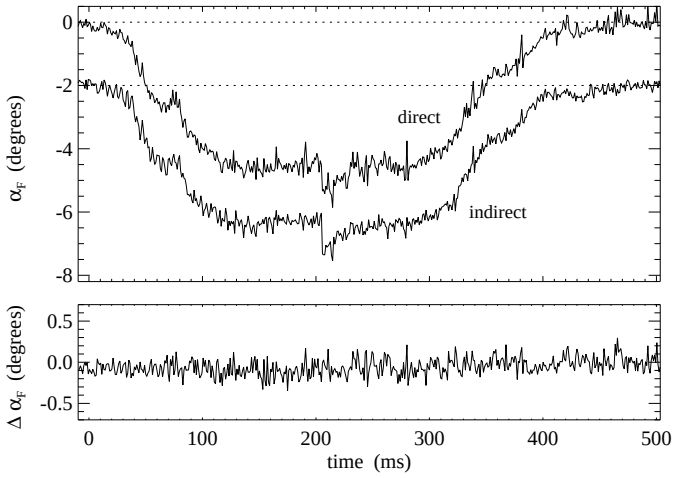

Figure 8. Faraday rotation of a single time trace from figure 7. In this case, the Faraday rotation has been derived both directly from the probe–probe mix and indirectly from the difference between the two probe–LO mixes. Again, one of the traces has been offset artificially. The bottom plot shows the difference between the two traces, without offset. Both methods yield identical results within the measurement accuracy.

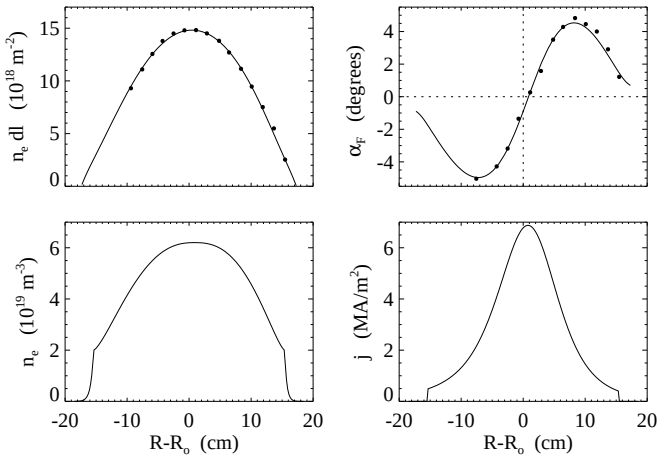

Figure 9. Line-integrated density profile and Faraday rotation profile for the discharge of figure 7, at 200 ms with a temporal resolution of 0.5 ms. From these measurements, both the density and the current density have been reconstructed using parametrized functions (see text), where $I_p = 130$ kA, $a = 0.154$ m, $q_a = 2.94$, $q_0 = 0.75$, $n_0 = 6.2 \times 10^{19}$ m^{-3}, $n_a = 2.0 \times 10^{19}$ m^{-3}, $\beta = 2.5$ and $\gamma = 1.4$.

possible density profiles during ohmic discharges. The current profile was assumed to be of the Kadomtsev type [12], with the q on axis as the only free parameter. Furthermore, a Shafranov shift has been assumed with a quadratic dependence on the radius of the flux surface. The displacement of the magnetic axis with respect to the last closed flux surface is fitted, and for this particular case found to be 9 mm.

Figure 10 demonstrates the capability of the diagnostic to determine the plasma magnetic axis. In the top plot, both the centre of the last closed flux surface, as derived from a saddle

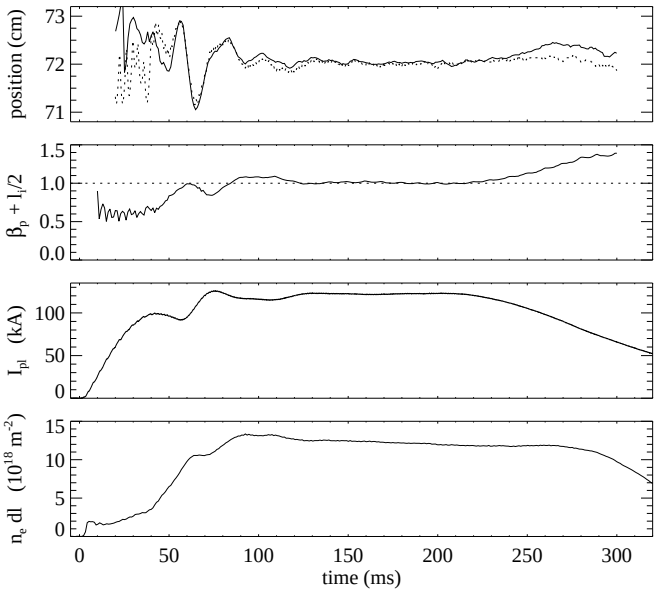

Figure 10. Illustration of the discrepancy between the magnetic axis as determined with saddle coils (dashed), and from the Faraday rotation data (solid). Because of inaccuracies in the absolute calibration of both measurements, the plasma positions were shifted to coincide when $\beta_p + l_i/2$ equalled unity. In this way, the deviations between the two signals become clearly visible. Note that these deviations are correlated with changes in $\beta_p + l_i/2$, which is a measure of the magnitude of the Shafranov shift. During the first 40 ms of the discharge, the density is relatively low, and hence the accuracy of the magnetic axis determination is less.

coil measurement, and the position of the magnetic axis derived from the Faraday rotation are given. The signals are shifted to overlap during the flat-top phase of the discharge, where $\beta + l_i/2$ equals unity. From the data it is obvious that, once $\beta + l_i/2$ deviates from its flat-top value, the Shafranov shift is also either increased or decreased, consistent with theoretical expectations.

6. Summary

In this paper a new polarimetric measurement scheme has been presented, involving two orthogonally polarized probing beams at slightly offset laser frequencies. The method involves separate phase demodulation of the three IF peaks associated with the mixing of the frequency-offset co-aligned probe beams and local oscillator. Only a single detector per spatial channel is required for high temporal resolution interferometric and polarimetric phase measurements. Unlike other processing methods, neither the interferometric nor the polarimetric phases are polluted by crosstalk. It has been demonstrated that the Faraday rotation angles are reliably conveyed using the new measurement principle provided the probing beams are sufficiently close to circularly polarized.

Acknowledgments

It is a great pleasure to acknowledge the expert technical advice on the construction of a triple far-infrared laser provided by Scott Burns.

The authors are indebted to the entire the RTP team, in particular to Frank Karelse and Theo Oyevaar, for their assistance in acquiring the presented data.

This work was performed as part of the research programme of the association agreement of Euratom and the 'Stichting voor Fundamenteel Onderzoek der Materie' (FOM), with financial support from the 'Nederlandse Organisatie voor Wetenschappelijk Onderzoek' (NWO) and Euratom.

References

[1] Donné A J H 1195 *Rev. Sci. Instrum.* **66** 3407–23
[2] Soltwisch H 1986 *Rev. Sci. Instrum.* **57** 1939–44
[3] Howard J 1993 *Infrared Phys*. **34** 175–89
[4] Kunz W and Dodel G 1978 *Infrared Phys*. **18** 769–72
[5] Dodel G and Kunz W 1978 *Infrared Phys*. **18** 773–6
[6] Rice B W 1992 *Rev. Sci. Instrum.* **63** 5002–4
[7] Barry S, Nieswand C, Bühlmann F, Prunty S L and Mansfield H M 1996 *Rev. Sci. Instrum.* **67** 1814–7
[8] Erickson R M, Forman P R, Jahoda F C and Roberts J R 1984 *IEEE Trans. Plasma Sci.* **PS-12** 275–80
[9] Soltwisch H 1993 *Plasma Phys. Control. Fusion* **35** 1777–86
[10] Rommers J H 1996 *Thesis* University of Utrecht *to be published*
[11] Hutchinson I H 1987 *Principles of Plasma Diagnostics* (Cambridge: CUP) p 118–21
[12] Kadomtsev B B 1987 *Phil. Trans. R. Soc. Lond. A* **322** 125–31